ECG Signal Classification Method for Double-threshold Segmented Sparse Representation

Ming-Xuan Yan, Jia-Cheng Zhou, Jia-Min Huang, Yu-Jie Jiang, Xiao-Jun Zhang * and Zhi Tao*

Abstract—**In this paper, we propose a method of extracting features from ECG signals based on the sparse representation of double-threshold Stagewise orthogonal matching Pursuit. First, the ECG signal was de-noised and then the K singular value decomposition algorithm (KSVD) was used to iterate the ECG data set to obtain a supercomplete dictionary of ECG signals. Then, through the double-threshold Stagewise orthogonal matching Pursuit, a sparse atomic matrix with the best reconstruction effect is finally selected to obtain the characteristics of ECG signals. Normal, atrial fibrillation, and ventricular fibrillation ECG signals from MIT's ECG Signal Database (MIT-BIH) were used to evaluate the proposed method. Experimental results show that in the binary classification experiment, the comprehensive recognition rate of the proposed algorithm for normal ECG signals, ventricular fibrillation and atrial fibrillation is 93.96%, 1.26% higher than that of CNN, and 3.99% higher than that of wavelet transform. Meanwhile, the five parameters of the proposed algorithm, such as comprehensive Kappa and comprehensive root relative square error, are the best. In addition, this paper carries out three-classification recognition of normal, atrial fibrillation, and ventricular fibrillation signals. The average recognition rate of the proposed algorithm among the three classifiers is 89.17%. The average recognition rate is 3.2% and 6.67% higher than that of convolutional neural networks and wavelet transform, respectively. The experimental results show that the features extracted in this paper have high recognition performance for arrhythmia ECG signals.**

Index Terms—**Double-threshold location, Dictionary learning, orthogonal matching pursuit, Sparse representation**

I. Introduction

Cardiovascular diseases are the leading cause of death worldwide. Since the beginning of the 21st century, aging has intensified, and the incidence rate of cardiovascular diseases has skyrocketed. Clinical cardiovascular diseases are often accompanied by arrhythmia, among which atrial fibrillation and ventricular fibrillation can lead to stroke and cardiac arrest. Therefore, timely and accurate detection of the type of arrhythmia is urgent and necessary. Electrocardiogram (ECG) signal detection is advantageous because it is non-invasive, with a high recognition rate and rapid recognition. As such, it has become the most commonly used diagnostic tool for cardiovascular diseases. Because of the complexity and diversity of human ECG signals, however, it is difficult to classify them. The sparse representation of ECG signals has become a new breakthrough point for the study of ECG signals.

Traditional methods of extracting features from ECG signals include hardware detection methods, template-matching methods, wavelet change methods, and morphological analysis. Hardware detection mainly uses a peak voltage detection meter and voltage comparator to detect R waves. However, this method is greatly affected by the environment and the characteristics of the measuring devices. The template-matching method involves recognizing images of ECGs and taking existing signal features, such as R waves and QRS wave groups, as a template feature vector. This method extracts the feature vector that matches the position of the template feature vector from the image to be tested for a comparative experiment, calculates the difference between the feature vector obtained from the recognition image and the template feature vector, and identifies the image wave group according to the difference [1]–[2]. But template matching requires establishing a standard template library in advance, and this requires a large amount of probability distribution calculations, which are easily subjected to interference from external noise that can lead to misjudgments. The wavelet change method uses a wavelet transform to decompose ECG signals and obtain time domain information and high-order statistics of the ECG signals [3]–[6]. However, this method relies heavily on carefully selected features, making it difficult to handle multi-class classification tasks. With morphological analysis, feature extraction and analysis of ECG signals are carried out according to the QRS wave group, T waves, R waves, and other information provided by ECG signal waveforms [7]–[8]. Yet this method requires manual feature extraction. As such, the designer much have ample experience for the method to be effective. In addition, when there is a lot of noise in the original signal or the morphological characteristics of the ECG signal are not obvious, information may be omitted.

In recent years, the development of artificial intelligence and deep learning has provided a method by which deep features can be automatically learned, avoiding the influence of artificial designs on classification efficiency. Deep learning can now effectively replace traditional ECG signal feature extraction algorithms. Deep learning methods applied

Manuscript received December 28, 2022; revised September 1, 2023.

Mingxuan Yan is a postgraduate student of Soochow University, Suzhou 215000, China. (e-mail:1923403032@ stu.suda.edu.cn).

Jiacheng Zhou is an undergraduate student of Soochow University, Suzhou 215000, China. (e-mail:2023402008@ stu.suda.edu.cn).

Jiamin Huang is an undergraduate student of Soochow University, Suzhou 215000, China. (e-mail:2023402015@ stu.suda.edu.cn).

Yujie Jiang is an undergraduate student of Soochow University, Suzhou 215000, China. (e-mail:2123401010@ stu.suda.edu.cn).

Xiaojun Zhang is an associate professor of Soochow University, Suzhou 215000, China (corresponding author to provide e-mail: zhangxj@ suda.edu.cn).

Zhi Tao is a professor of Soochow University, Suzhou 215000, China (corresponding author to provide e-mail: taoz@suda.edu.cn).

to ECG classification and recognition include convolutional neural networks (CNNs) [9]-[13], decision trees and support vector machines [14-15], k-nearest neighbors [16], CNNs in combination with long short-term memory [17]-[21], and recurrent neural networks. Such methods have demonstrated good performance at signal classification. Deep learning methods use a deep neural network to extract the features of ECG signals and determine signal categories. However, deep learning requires considerable data and computing resources.

In what follows, we propose a feature extraction method ,which is called double-threshold Stagewise orthogonal matching Pursuit (DSWOMP), for ECG signals based on sparse representation. A wavelet transform is first used to filter out baseline drift and electromyographic noise in the ECG signals. Then, the Butterworth low-pass filter is used to filter out high-frequency noise in the signals, and the processed signals are iterated using the K-singular-value decomposition algorithm to obtain a supercomplete dictionary of normal, ventricular fibrillation, and atrial fibrillation ECG signals. Using this dictionary, a stagewise orthogonal matching pursuit algorithm is used to reconstruct the ECG signals. The sparse atomic matrix with the best reconstruction effect is then selected through the threshold parameters of the double-threshold positioning method, and the sparse atomic matrix of each signal is taken as the feature of the signal.

II. Preprocessing Based On Wavelet Transform

ECG signals collected by machines always have electromyographic noise caused by the human body itself and baseline drift caused by machine hardware extraction. This noise seriously affects the extraction of ECG signal features. Therefore, we applied filtering operations on the ECG signals collected before generating data sets. The function of the wavelet transform is to decompose the signal into a series of wavelet functions. Because of its excellent performance in both the time and frequency domains, the wavelet transform can carry out multi-scale subdivisions of signals through scaling and translation operations. As such, it is often used in signal processing. Because of its ability to subdivide time at both high and low frequencies—that is, it can automatically adapt to the analysis of time-frequency signals—we used the wavelet transform to reduce the noise in ECG signals. The scale coefficient of the wavelet transform is expected to reduce some noise in ECG signals. The definition of the wavelet transform is as follows:

$$WT_{\mathrm{f}}(a,b) = < f(t), \varphi_{a,b}(t) > \tag{1}$$

The db5 wavelet cluster is selected from among many wavelets to decompose the collected ECG signals, which are decomposed into eight layers. First, we consider the detailed coefficient and approximate coefficient of ECG signal decomposition. The first and second layers of the detailed coefficient of ECG decomposition contain most of the high-frequency noise in the ECG signal. The eighth layer of the approximate coefficient contains the baseline drift noise in the signal. The ECG signal itself is not highly correlated with the first, second, and eighth layers of the approximate coefficient. Therefore, we set the first and second layers of the detailed coefficient to zero to eliminate high-frequency noise in the ECG signal. To eliminate baseline drift noise in ECG signals, we used the above method to set the eighth layer of the approximate coefficient in the decomposed signals to zero. Finally, the ECG signal was reconstructed according to the processed approximate coefficient to obtain a relatively clean ECG signal.

However, the wavelet transform only filters out high-frequency noise and baseline drift in the ECG signal. Other EMG noise remains in the ECG signal, resulting in considerable jitter. In order to obtain a smoother ECG signal, the Butterworth low-pass filter is used to extract the envelope of the ECG signal. The energy of ECG signals is mainly concentrated in the range of 5 – 20 Hz. We selected the second-order Butterworth low-pass filter with a cut-off frequency of 15 Hz, according to the energy of ECG signals. The signal de-noised with this filter is close to the standard ECG signal.

Normalization can increase the contrast between signals. Thus, we used normalization to process the ECG signal after extracting the envelope. The amplitude of the ECG signal was limited to [-1, 1]. The normalization formula is as follows:

$$\tilde{F}(n) = F(n) / F_{\max} \tag{2}$$

where F(n) is the signal after envelope processing, and Fmax is the maximum value of the signal after envelope processing.

We selected a normal signal to show the effect of noise reduction. Figure 1 provides diagrams to compare the original signal to the signal after wavelet transform de-noising, envelope extraction, and normalization . In the figure, the abscissa is the number of sampling points of the ECG signal, and the ordinate is the signal amplitude.

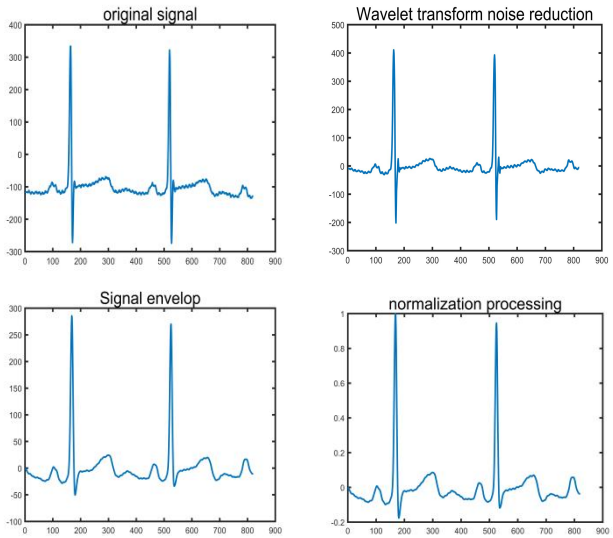

Fig. 1. Comparison of the original signal, the signal after noise reduction, and the signal after normalization

III. K-Singular-Value Decomposition Algorithm

A. Sparse Representation

Sparse representation mainly consists of finding a suitable dictionary for non-sparse samples, so that the samples can be converted into a linear combination of several nonlinear correlation vectors in the dictionary, thus simplifying the learning task, reducing the complexity of the model, and

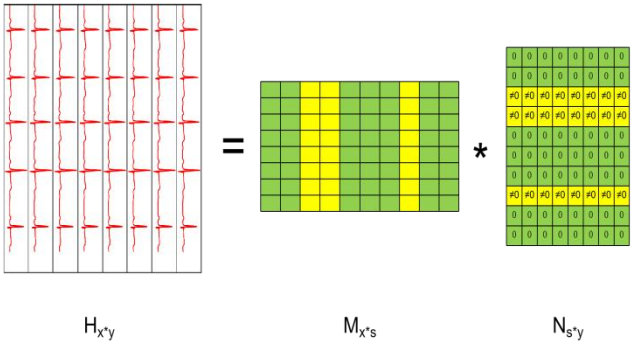

Fig. 2. Schematic diagram of sparse representation

reducing the calculation time. The process of finding a dictionary is called "dictionary learning". That is, the process of selecting sparse atoms in the dictionary to represent the original sample by sparse coding is the process of solving sparse atoms. The core idea of sparse representation is to find a suitable dictionary for the samples of ordinary dense representation and convert the samples into a suitable sparse representation—that is, to express most or all of the original signals with a few linear combinations of basic signals. Its schematic diagram is shown in Fig. 2.

Suppose we use a matrix H_{x*y} to represent the data set—that is, a set of signals in a total of y columns, each of which represents an ECG signal, and x rows, each of which represents a characteristic attribute of a sample. In general, the sample matrix is dense. That is, most of the elements are non-zero. The meaning of sparse representation is to find two matrices to reconstruct the original signal. Specifically, we find a dictionary matrix M_{x*s} and a sparse matrix N_{s*y} , so that $M_{x*s} * N_{s*y}$ can reproduce the sample matrix H_{x*y} as much as possible, and each column of sparse vectors of N_{s*y} can be as sparse as possible. N_{s*y} is the sparse representation of the sample matrix H_{x*y}:

$$H_{x*y} = M_{x*s} * N_{s*y} \tag{3}$$

B. Sparsity Analysis of ECG Signals

ECG signals are complex narrow-band signals concentrated at low frequencies. Most of their energy is concentrated in the frequency range of 0.5–30 Hz. In the time domain, the ECG signals show the non-stationary characteristics of quasi-periods, and the signals between each period are very similar. These two characteristics mean that ECG signals are compressible and strongly correlated with each other. In addition, ECG signal waveforms between people show roughly the same waveforms on the whole, due to the fitness and cardiovascular differences between people, although there are differences in the details. If there are cardiac arrhythmias caused by cardiovascular disease, there will be a big difference in the performance of the ECG signal. In this paper, the redundancy of signals is removed to construct a sparse dictionary of ECG signals.

C. K-Singular-Value Decomposition Algorithm

The sample matrix H_{x*y} is divided into a group of y vectors with x elements in each group of vectors; i.e., y $H_{x*y} = [h_1, h_2, \cdots, h_y]$. Similarly, the sparse matrix N_{s*y} is changed to $N_{s*y} = [n_1, n_2, \cdots, n_y]$, and the 0-norm, namely $\|\cdot\|_0$, is introduced to make N_{s*y} as sparse as possible. Thus, $\|n\|_0$ represents the sparsity of the sparse coefficient n, and this mathematical formula represents the number of non-zero coefficients of the sparse coefficient n. In the research, the data are expected to be as sparse as possible; that is, H is as small as possible. To solve the sparse representation, it can be converted into the following convex optimization problem:

$$\hat{n}_i = \arg\min \| n_i \|_0 \quad \text{s.t. } h_i = M_{x*s} n_i \quad i = 1,2,\cdots,n \tag{4}$$

If the sparse vector in each column of N_{s*y} must be k-sparse, then the number of non-zero elements of the coefficient vector in each column of N_{s*y} is k, and k is the sparsity. Equation (2) can be transformed into:

$$\hat{n}_i = \arg\min \| h_i - M_{x*s} n_i \|_2^2 \quad \text{s.t. } \|n_i\|_0 \le k \quad i = 1,2,\cdots,n \tag{5}$$

Although 0-norm minimization can derive a nearly perfect analytical solution, the solution of 0-norm minimization is still problematic. It is later found that 1-norm minimization has a common solution with 0-norm minimization under certain conditions, while 1-norm minimization has no problem. Therefore, the above convex optimization problem can be written as:

$$\hat{n}_i = \arg\min \| h_i - M_{x*s} n_i \|_2^2 \quad \text{s.t. } \|n_i\|_1 \le k \quad i = 1,2,\cdots,n \tag{4}$$

K-singular-value decomposition includes the following steps. First, the dictionary is initialized, whereby m samples are randomly selected from the data set H as the initial dictionary, which is denoted $M = [m_1, m_2, \cdots, m_s]$. Second, the sparse matrix is initialized. According to the initial predefined dictionary, the orthogonal matching tracking algorithm is used for sparse decomposition of the sample matrix H, and sparse coefficient matrix $N = [n_1, n_2, \cdots, m_y]$ is obtained. Third, the dictionary is updated by fixing the sparse coefficient matrix N and updating the atoms in the dictionary M column by column:

$$\| H - MN \|_2^2 = \| (H - \sum_{j \ne k} m_j n_j^T) - m_k n_k^T \|_2^2 = \| E_k - m_k n_k^T \|_2^2 \tag{6}$$

where m_j represents the j-th column in dictionary M, n_j^T represents the j-th row in N, and E_k represents the error after removing m_k. When updating the dictionary, we first update the k-th atom mk in the supercomplete dictionary M, calculate the error matrix E_k, select the index set that is not 0 in the k-th row vector n_j^T of the sparse coefficient matrix, and define the index set:

$$w_k = \{ i \mid 1 \le i \le y, n_k^T(i) \ne 0 \} \tag{7}$$

IV. Double-Threshold Positioning Stagewise Orthogonal Matching Pursuit Algorithm

Stagewise orthogonal matching pursuit is a greedy algorithm derived from the orthogonal matching algorithm. It aims to improve the accuracy of orthogonal pursuit algorithm reconstruction and improve the computing efficiency. OMP eliminates the atom with the greatest correlation with the

sample signal in each iteration, and ensures that the eliminated signal is orthogonal to the eliminated vector, and that the eliminated vector does not need to be repeatedly calculated in each subsequent iteration. However, it is difficult for this algorithm to ensure the global optimum of each search result, and there may be sub-optima. Stagewise orthogonal matching pursuit algorithm can add a threshold value, select the signal with a better effect in the residual signal, and send it to the next iteration, ultimately achieving the effect of improving the signal reconstruction rate. However, the threshold value of the algorithm needs to be set manually. If the threshold value is set improperly, the signal may be overprocessed or underprocessed. In this paper, a feature extraction method of ECG signals based on double-threshold positioning and stagewise orthogonal matching pursuit is proposed.

A. Double-Threshold Location Algorithm

The threshold value of the stagewise orthogonal matching pursuit algorithm is adjustable between 0 and 1. Traversing from 0 to 1 at steps of 0.01, the iteration number of stagewise orthogonal matching pursuit is set to 20 times. Then, the reconstruction error rate of the original signal is calculated under different threshold values, that is, the difference between the original signal and the reconstructed signal. This difference is divided by the original signal value. The calculation is given as follows:

$$H_{sum} = \sum_{\mathrm{j}}^{\mathrm{x}} \sum_{i}^{\mathrm{y}} \frac{H(j,i) - H\_c(j,i)}{H(j,i)} \tag{8}$$

In (8), H_{sum} is the reconstruction error rate, $H(j,i)$ is the original signal, and $H\_c(j,i)$ is the reconstructed signal.

The 100 reconstruction error rates were analyzed, the index of the minimum reconstruction error rate was selected, and the interval of [-5,5] was set to zero. The minimum reconstruction error rate after screening was selected again, and its index was recorded. The difference between the second index and the first index was then judged. If the difference was 5, the first index was recorded. By default, it is the optimal threshold of the stagewise orthogonal matching pursuit algorithm. If the difference between the second index value and the first index value is greater than 5, there is a suboptimal value. In that case, it is necessary to make a second threshold judgment. The threshold values of the two indexes are respectively followed by 20-fold segmental orthogonal matching tracking. After calculating segmental orthogonal matching tracking every 20 fold, the loss rate is judged:

$$H_{suml} = \sum_{\mathrm{i}}^{\mathrm{x}} (H(:,i) - H\_c(:,i))\text{^}2 \tag{9}$$

The sum of the residual squares of each column of the entire sample matrix is calculated to determine whether the loss rate is approximately 0. If it is approximately 0, it is recorded as a successful reconstruction, and the entire sample matrix is traversed to determine the success rate of sample reconstruction:

$$\theta = \frac{L_{\mathrm{s}}}{L} \tag{10}$$

In (10), Ls is the number of successful sample reconstruction columns, and L is the number of total sample columns. The index value with the higher sample reconstruction rate calculated by the two index values is the optimal threshold value of the stagewise orthogonal matching pursuit algorithm.

B. Double-Threshold Stagewise Orthogonal Matching Pursuit Algorithm

Because the traditional SWOMP algorithm needs to set the threshold artificially, the dual-threshold positioning method and the SWOMP algorithm are combined to form the DSWOMP algorithm, which is applied to ECG signal feature extraction. The algorithm is shown as follows:

Algorithm 1 DSWOMP algorithm

Input：H (Sample matrix of ECG signal), M (Overcomplete dictionary matrix)，L (Initial sparse atomic number)

Output：E (Sparse coefficient matrix)

Step 1：Assign the residual matrix, make $\mathrm{r}_0 = \mathrm{H}$.

Step 2：Define the update dictionary matrix x_0， The matrix of reconstruction the error rate y_0。

Step 3：Initialize the threshold Th←0, The number of iterations P←0，The index $Z_{\mathrm{i}} \leftarrow \Phi$ 。

Step 4：

for Th <= 1 **do**

(a): Add 0.1 to the threshold value Th ← Th + 0.1。

(b):

for P<=20 **do**

(1): Calculate the inner product of dictionary matrix and residual matrix.

$$\mathrm{S} \leftarrow \mathrm{abs}[\mathrm{M}^{\mathrm{T}} \mathrm{r}_{\mathrm{i-1}}]。$$

(2): The atoms in S larger than Th are used as the index J_{i} to construct the atom set.

$$J_{\mathrm{i}} \leftarrow \mathrm{find}(S >= \max(S) * Th),$$

(3): Update the index Z_{i}。

$$Z_i \leftarrow Z_i \cup J_i$$

(4)： Update the dictionary matrix x_{i} by index Z_{i}

(5): The least squares method is used to solve the sparse coefficient matrix E_i

$$\hat{E}_i \leftarrow \arg\min \| \mathrm{H} - \mathrm{x}_i E_{i-1} \|_2$$

(6): Update the residual matrix r_{i}

$$\mathrm{r}_{\mathrm{i}} \leftarrow \mathrm{H} - \mathrm{x}_{\mathrm{i}}^{\mathrm{L}} \mathrm{E}_i^L$$

end for

(c) : The number of iterations increases by one

$P \leftarrow P+1$

(d) : According to Equation (7), the reconstruction error rate is calculated and stored in y_0

end for

Step 5： Obtain the minimum value of y_0 and its position index s, set the field of s[-5,5] to zero, and generate y_1.

Step 6： Obtain the minimum value of y_1 and its position index d, and obtain the threshold m according to the two minimum values.

$m \leftarrow |s-d|$.

Step 7：

If m = 5, **then**

do

(a) : Obtain the optimal threshold value Th

$Th \leftarrow s*0.01$。

(b) : The sparse coefficient matrix is obtained according to the threshold value E_i;

else

(a) : Get index s, The threshold value of d;

(b) : The success rate of reconstruction was calculated according to Equations (7) and (8);

(c) : Select the one with the higher success rate as the best threshold value, and obtain the sparse coefficient matrix E_i;

end if

The three kinds of ECG signals are de-noised by wavelet transform, and the EMG noise and baseline drift of ECG signals are filtered. The ECG signal matrix is constructed with the processed signals as shown in Figure 1, and the ECG signal matrix is sent into the K-singular-value decomposition algorithm. After iteration, an overcomplete dictionary of the ECG signal sample matrix is obtained. Finally, the ECG signal matrix and the overcomplete dictionary matrix are sent together to the double-threshold stagewise orthogonal matching pursuit algorithm to obtain the sparse matrix under the optimal threshold. Finally, the sparse atomic matrix of each signal is used as the characteristic of the signal. The flowchart of the algorithm for segmented sparse representation of double-threshold values is shown in Fig. 3.

V. Introduction to The Classifier

A. Decision trees

Decision trees are named for their shape. This classifier generates tree-like flow diagrams based on the "if - then" judgment principle. Decision trees consist of three parts: test nodes, branches, and leaf nodes. Each test node represents an attribute judgment on the data. The first test node of the tree, the topmost node of the tree, is also called the root node. The attribute tests at the root node are usually the tests that we think will have the most impact on the final classification result. A branch is the output of each test node, which leads either to the leaf node or to the next test node for the next round of property testing.

Most decision-tree algorithms are top-down divide-and-conquer management methods. The impact of test nodes on leaf nodes decreases from top to bottom, and the root node is the node with the highest correlation to the leaf nodes. Another important part of a decision tree is the attribute selection measure of the test node — that is, the setting of the "if" decision condition. There are three popular methods for setting the attribute decision condition: the information gain, information gain rate, and Gini index.

B. Random forests

In this paper, random forests are used to classify the features extracted by the DWT, CNN, and proposed algorithm. The random forests algorithm adds randomness to a decision tree to improve its performance. Random forests involve integrated learning, where the basic idea is to use a large number of decision trees — that is, classifiers with relatively weak classification ability—as base classifiers, and to obtain classifiers with better predictions by combining these decision trees.

The classifier uses a meta-learning algorithm that can be divided into a combinator and a decision. The specific working process of the combinator is as follows: among X original samples, c samples are selected by random sampling, and these c samples are formed into a new sample set that is included in the original sample set. This operation is repeated Y times so that there are Y sample subsets of the original samples in the classifier. Each sample subset is sent to the basic classifier. The total number of test attributes is denoted as M, and m are randomly selected from the total number of test attributes, where m is less than M. Then, Y classifiers are predicted and Y test results are obtained. The following is the work of the decision in the meta-learning algorithm. Random forests are used for classification, so the decision adopts the voting method to determine the final category. That is, the result that appears the most times among the Y results is the classification result of the algorithm we want.

C. RandomCommittee

RandomCommittee and random forests are both based on a meta-learning algorithm, so RandomCommittee also involves integrated learning with several basic classifiers. The difference between this classification algorithm and the random forests classification method is that the basic classifier of random forests is a fixed decision tree, and the RandomCommittee classification algorithm can be changed: we can choose a basic decision tree, the naive Bayes classifier,

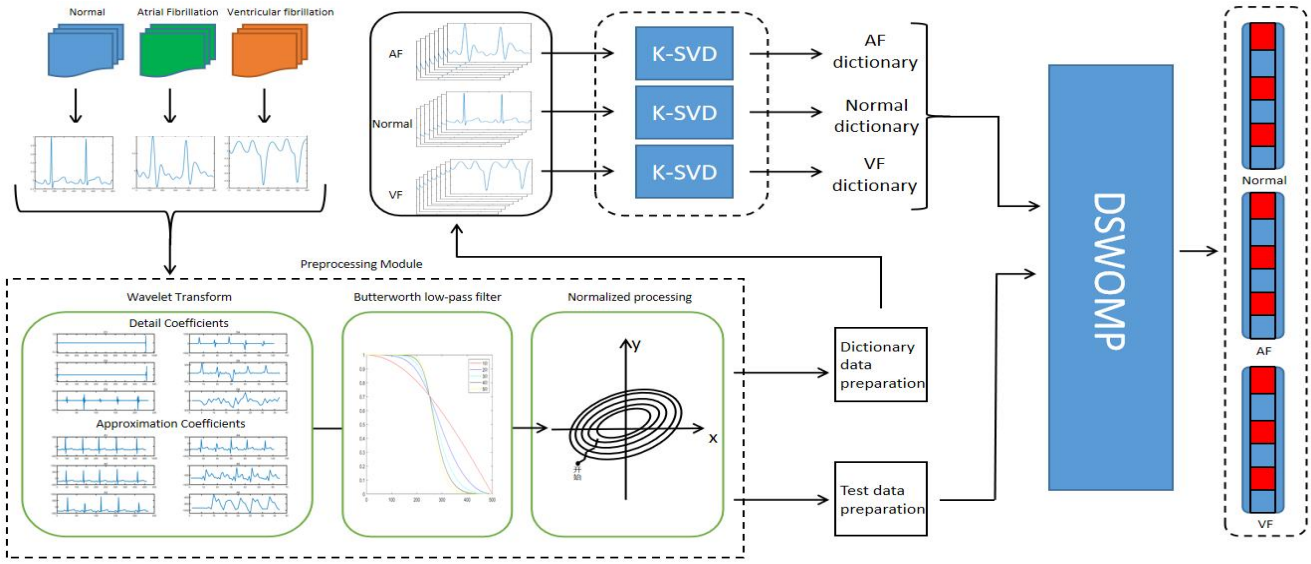

Fig. 3. Flowchart of double-threshold segmented sparse representation algorithm

a multi-layer perceptron neural network, etc. We opted for the IBK, a classifier based on the k-nearest neighbors algorithm, as the basic classifier.

The k-nearest neighbors algorithm involves using a new sample as the data training set. The distance between the sample and the surrounding training set samples is then calculated, and the k samples closest to the new sample are marked. Finally, the category of the new sample is determined according to the principle of minority obedience.

D. BayesNet

BayesNet's model is a directed acyclic graph that consists of two parts: nodes and directed edges. The correlation degree of the parent node to the child node is evaluated by calculating the conditional probability. The node represents a random variable corresponding to the ECG characteristics input in this paper, and the directed edge is the connection between the two nodes. When the node is the initial node—that is, with no parent node—the prior probability is used for information expression. By calculating the conditional probability between each node, the network obtains the probability of the final label and realizes the classification of the database. The specific process is to send to the network the data to be measured, match the features to be measured with the existing network, calculate the conditional probability of the nodes, and obtain the prediction label.

VI. Experimental Results and Discussion

The ECG signal in this experiment comes from the ECG Signal Database (MIT-BIH) provided by the Massachusetts Institute of Technology. The three ECG signal databases are the normal sinus rhythm database, atrial fibrillation database, and ventricular fibrillation database[22].

All databases are in “dat” files in dual-channel data, among which the data waveform of the first channel is more commonly used than that of the second channel. Therefore, we adopted the MIT-BIH ECG signal data of the first channel in this study.

The MIT-BIH atrial fibrillation database consists of the long-term electrocardiogram records of 25 human subjects with atrial fibrillation at a sampling rate of 250 Hz and a resolution of 12 bits. The database was collected at the Beth Israel Hospital in Boston. A normal sinus rhythm database and atrial fibrillation database were collected from a hospital and consisted of five men aged 26 to 45 years and 13 women aged 20 to 50 years at a sampling frequency of 128 Hz with a sampling accuracy of 11 digits. The ventricular fibrillation database was based on the sudden cardiac death Holter electrocardiogram database, which was originally collected by Scott Greenwald when he was at MIT. It was collected from 23 patients with ventricular fibrillation. First, the ECG signal samples obtained in the data set were up-sampled. The normal ECG signal sample was raised from 128Hz to 250Hz. Uniform sampling rate for more reliable data. In order to prevent the large difference in the number of samples from causing the classifier to prefer samples with a large number of samples, this paper selects 80 samples of each ECG signal sample after sampling, and 240 samples of the three types of signals in total.

The detailed information of the three databases is shown in Table I.

TABLE I
Data Information Table

		Gender			Age	Sampling parameter	
	Total	Male	Female	Unknown	Range	Sampling rate	Sampling accuracy
Normal	18	5	13	-	20-50	128	11
AF	25	-	-	25	-	250	12
VF	23	13	8	2	17-82	250	-

The data samples in the MIT-BIH database were identified, read, and classified by the editor, and the three types of ECG signal morphological results were obtained, as shown in Fig . 4.

ECG signal samples are sent to the K-SVD algorithm to generate an overcomplete dictionary through ECG signal reconstruction. After iteration, the reconstruction failure rate curve of the overcomplete dictionary generated by the K-SVD algorithm is shown in Fig. 5.

ECG signal samples are sent to the K-SVD algorithm to generate an overcomplete dictionary through ECG signal reconstruction. After iteration, the reconstruction failure rate

curve of the overcomplete dictionary generated by the K-SVD algorithm is shown in Fig. 5.

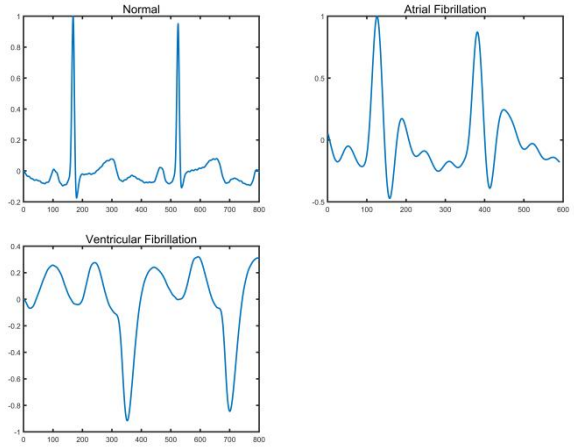

Fig. 4. Morphological classification of three types of ECG signals

As can be seen from Fig. 5, the reconstruction failure rate of the K-SVD algorithm in this paper during the generation of the overcomplete dictionary decreases from 26.5% to 12% after iteration, greatly improving the completeness of the overcomplete dictionary.

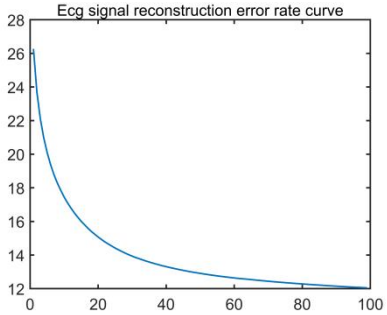

Fig. 5. ECG signal reconstruction error rate curve

Common ECG signal feature extraction algorithms include morphological feature extraction based on wavelet transforms and feature extraction based on the convolutional neural network. We applied these two methods to the database for feature extraction. The two methods and the ECG features extracted by the proposed method were verified by 10-fold cross-validation, to ensure the accuracy of the test system. All the characteristic data were divided into ten parts. One part was selected as the test set and the other nine parts as the training set. After a test was completed, the remaining nine parts were selected as the test set in turn, and the remaining nine parts of each non-test set were selected as the training set. The corresponding accuracy rate was recorded, with the average of ten tests as the final result. In this way, the probability of error is greatly reduced and the accuracy of test results is guaranteed. Three classification methods, RandomForest, RandomCommittee, and BayesNet, were used for a pair-to-pair classification comparison of the features extracted by the DWT, CNN, and DSWOMP algorithms. In this study, we used the number of correctly classified instances, root relative squared error, relative absolute error, root mean squared error, mean absolute error, and Kappa to analyze the experimental results of the classifier. These six parameters aptly reveal the classification effect of the extracted features in the classifier. The correctly classified instances and the Kappa are such that the larger the value, the better the classification. The root relative squared error, relative absolute error, root mean squared error, and mean absolute error are such that the smaller the value, the better the classification effect of the extracted ECG features in this classifier. Since the DWT, CNN, and DSWOMP algorithms output more parameters in the three classifiers, we focused on analyzing the mean value of the three feature extraction algorithms in the three classifiers—that is, to obtain the mean value of each parameter obtained by each feature extractor after classification by the three classifiers.

TABLE II
CLASSIFICATION RESULTS OF NORMAL ECG SIGNALS AND VF SIGNALS

		Classification unit			
		RandomForest	RandomCommittee	BayesNet	Mean
DWT	Correctly classified Instances	95%	93.13%	98.13%	95.42%
	Kappa	0.90	0.86	0.96	0.91
	Mean absolute error	0.06	0.07	0.02	0.05
	Root mean squared error	0.18	0.23	0.14	0.18
	Relative absolute error	11.87%	13.94%	4.09%	9.97%
	Root relative squared error	36.74%	45.81%	27.72%	36.76%
CNN	Correctly classified Instances	98.75%	98.75%	98.75%	98.75%
	Kappa	0.98	0.98	0.98	0.98
	Mean absolute error	0.01	0.01	0.01	0.01
	Root mean squared error	0.11	0.11	0.11	0.11
	Relative absolute error	2.5%	2.5%	2.5%	2.5%
	Root relative squared error	22.25%	22.36%	22.36%	22.36%
DSWOMP	Correctly classified Instances	100%	100%	100%	**100%**
	Kappa	1.00	1.00	1.00	**1.00**
	Mean absolute error	0.005	0.00	0.005	**0.01**
	Root mean squared error	0.03	0.00	0.02	**0.03**
	Relative absolute error	2.15%	1%	0%	**1.05%**
	Root relative squared error	5.23%	5.48%	0%	**3.57%**

Normal ECG signals and ventricular fibrillation signals were classified and analyzed. The classification results are shown in Table II.

The confusion matrix of the normal and ventricular fibrillation classifiers is shown in Fig. 6.

It can be seen from Table II that the average recognition rate of features extracted by DWT is 95.42% in RandomForest, RandomCommittee, and BayesNet, and the average recognition rate of features extracted by the CNN is 98.75% in the three classifiers. The average recognition rate of the features extracted by the proposed algorithm is 100%

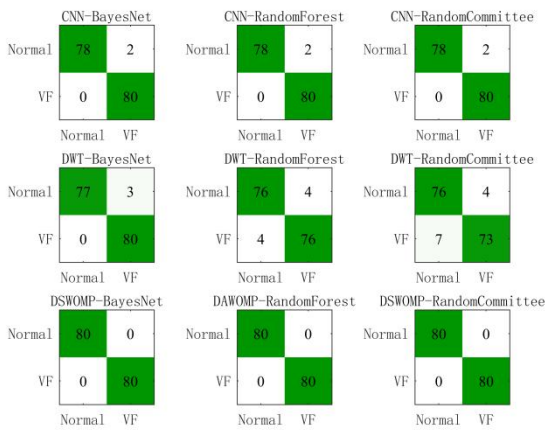

Fig. 6. Different machine learning confusion matrices for normal and ventricular fibrillation

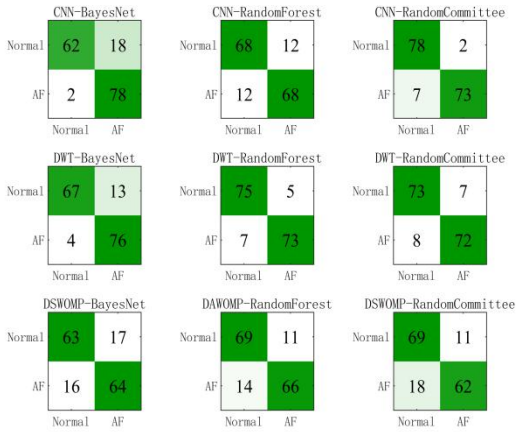

Fig. 7. Different machine learning confusion matrices for normal and atrial fibrillation

in the three classifiers. The proposed algorithm has absolute advantages in the feature extraction of normal and ventricular fibrillation signals. The kappa mean value of features extracted by the proposed algorithm (kappa value = 1) is also

TABLE III
CLASSIFICATION RESULTS OF NORMAL ECG SIGNALS AND AF SIGNALS

		Classification unit			
		RandomForest	RandomCommittee	BayesNet	Mean
DWT	Correctly classified Instances	92.5%	90.63%	89.38%	90.84%
	Kappa	0.85	0.81	0.78	0.81
	Mean absolute error	0.15	0.13	0.11	0.13
	Root mean squared error	0.25	0.27	0.31	0.28
	Relative absolute error	30.38%	26%	23.04%	26.47%
	Root relative squared error	50.22%	54.77%	62.44%	55.81%
CNN	Correctly classified Instances	85%	81.25%	87.5%	84.58%
	Kappa	0.70	0.63	0.75	0.69
	Mean absolute error	0.18	0.18	0.13	0.16
	Root mean squared error	0.34	0.37	0.35	0.35
	Relative absolute error	36.04%	36.13%	25.19%	32.45%
	Root relative squared error	69.98%	74.82%	70.71%	71.84%
DSWOMP	Correctly classified Instances	84.38%	81.88%	79.38%	**81.88%**
	Kappa	0.69	0.64	0.59	**0.64**
	Mean absolute error	0.29	0.26	0.24	**0.26**
	Root mean squared error	0.35	0.36	0.41	**0.37**
	Relative absolute error	57.26%	51.38%	47.90%	**52.18%**
	Root relative squared error	70.93%	72.41%	82.63%	**75.32%**

TABLE IV
CLASSIFICATION RESULTS OF VF SIGNALS AND AF SIGNALS

		Classification unit			
		RandomForest	RandomCommittee	BayesNet	Mean
DWT	Correctly classified Instances	83.13%	81.25%	85.63%	83.34%
	Kappa	0.66	0.63	0.71	0.67
	Mean absolute error	0.21	0.2	0.15	0.19
	Root mean squared error	0.35	0.38	0.37	0.37
	Relative absolute error	41.84%	40.25%	29.21%	37.1%
	Root relative squared error	70.66%	76.72%	73.90%	73.76%
CNN	Correctly classified Instances	95%	94.38%	95%	94.79%
	Kappa	0.90	0.89	0.90	0.90
	Mean absolute error	0.08	0.07	0.05	0.07
	Root mean squared error	0.22	0.22	0.22	0.22
	Relative absolute error	15.55%	13.38%	10.00%	12.98%
	Root relative squared error	44.57%	44.58%	44.72%	44.62%
DSWOMP	Correctly classified Instances	100%	100%	100%	**100%**
	Kappa	1.00	1.00	1.00	**1.00**
	Mean absolute error	0.02	0.01	0.00	**0.01**
	Root mean squared error	0.04	0.04	0.00	**0.03**
	Relative absolute error	3.14%	2.00%	0.00%	**1.71%**
	Root relative squared error	8.28%	8.37%	0.00%	**5.55%**

the highest among the three classifiers. The mean values of the mean absolute error and root mean squared error of the features extracted by the proposed algorithm are the smallest in the three classifiers, at 0.005 and 0.02, respectively. The

mean relative absolute errors of the CNN, DWT, and the features extracted by the proposed algorithm with the three classifiers were 9.97%, 2.5%, and 1.05%, respectively. The average relative absolute error of the ECG features extracted by the proposed algorithm is the smallest, indicating that the features extracted by the proposed algorithm have the best effect on the classification of normal and ventricular fibrillation signals. By comparing the above table data, it is found that the average root relative squared error of the proposed algorithm is 3.57%, much smaller than that of the CNN algorithm (22.36%) and the DWT algorithm (36.76%).

Normal ECG signals and atrial fibrillation signals are classified and analyzed below, and the classification results are shown in Table III.

The confusion matrix of normal and atrial fibrillation classifiers is shown in Fig. 7.

It can be seen from Table III that the average recognition rate of the features extracted by DWT in the three classifiers is 90.84%, the average recognition rate of the features extracted by the CNN in the three classifiers is 84.58%, and the average recognition rate of the features extracted by the proposed algorithm is 81.88%. DWT has an advantage in the feature extraction of normal and atrial fibrillation signals. In addition, it can be seen from the above table that the feature extracted by the proposed algorithm is not as effective as the DWT algorithm through the five parameters of Kappa, root relative square error, relative absolute error, root mean square error and mean absolute error. The proposed algorithm is not effective at classifying normal and atrial fibrillation signals.

The classification of ventricular fibrillation signals and atrial fibrillation signals is analyzed below, and the classification results are shown in Table IV.

The confusion matrix of classifiers for ventricular fibrillation and atrial fibrillation is shown in Fig. 8.

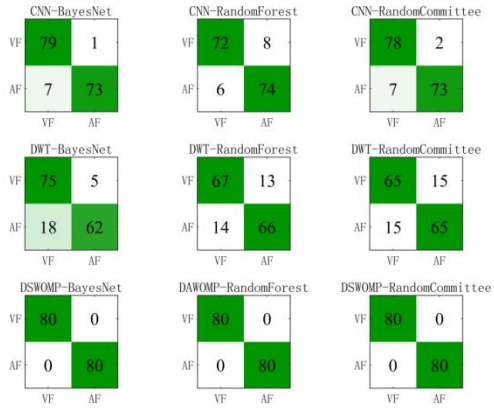

Fig. 8. Different machine learning confusion matrices for ventricular and atrial fibrillation

As can be seen from Table IV, the average recognition rate of the features extracted by DWT in the three classifiers is 83.34%, the average recognition rate of the features extracted by the CNN in the three classifiers is 94.79%, and the average recognition rate of the features extracted by the proposed algorithm in the three classifiers is 100%. The proposed algorithm still has absolute advantages in extracting features of ventricular fibrillation signals and atrial fibrillation signals, which is far superior to the features extracted by DWT. Moreover, the mean value of the Kappa of the features extracted by the proposed algorithm in the three classifiers is 1, higher than that of the CNN (0.9) and DWT (0.67). The root relative squared error, relative absolute error, root mean squared error, and mean absolute error were calculated by the three classifiers. The average values were 5.55%, 1.71%, 0.03, and 0.01, respectively. By comparing these four parameters with the values calculated by the CNN and DWT algorithms, it is found that the parameters of the proposed algorithm are the lowers, indicating that the proposed algorithm has the best effect in the binary classification of atrial fibrillation and ventricular fibrillation, outperforming the other two algorithms.

Through a comprehensive analysis of Tables I, II, and III, the features extracted by the proposed algorithm have excellent results in the binary classification of normal and ventricular fibrillation, as well as of ventricular fibrillation and atrial fibrillation. But they are slightly inferior to the other algorithms in the binary classification of normal and atrial fibrillation. To evaluate the algorithm further, we defined the comprehensive recognition rate as well as the comprehensive Kappa, comprehensive root relative squared error, comprehensive relative absolute error, comprehensive root mean squared error, and comprehensive mean absolute error. The results of the proposed algorithm are evaluated using these six parameters.The average recognition rate of the three DWT classifications is 95.42%, 90.84%, and 83.34%, respectively. The average recognition rate of the three classifications is 89.97%. The average recognition rates of the three classifications by the CNN were 98.75%, 84.58%, and 94.79%. CNN's overall recognition rate was 92.7%. The average recognition rates of the proposed algorithm were 100%, 81.88%, and 100% respectively, with an overall recognition rate of 93.96%. The comprehensive recognition rates of the CNN, DWT, and DSWOMP algorithms are shown in Fig. 9.

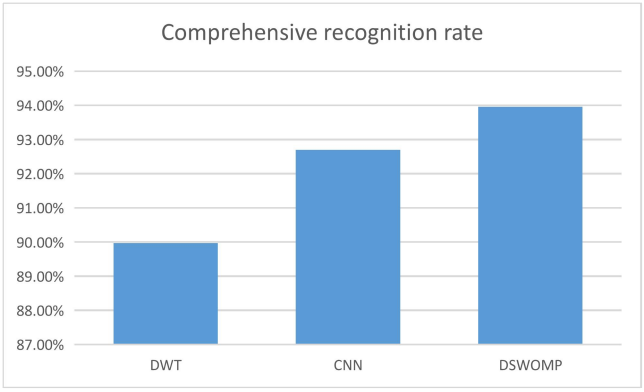

Fig. 9. Comprehensive recognition rate of CNN, DWT, and DSWOMP algorithms

The comprehensive Kappa, comprehensive root relative square error, comprehensive relative absolute error, comprehensive root mean square error, and comprehensive average absolute error of the proposed algorithm and the traditional ECG signal feature extraction algorithm are shown in Table V.

It can be seen from Table V that the comprehensive Kappa, comprehensive root-mean-square error, comprehensive relative absolute error, comprehensive root-relative square error, and comprehensive average absolute error calculated by the algorithm in this paper have the best results, and only

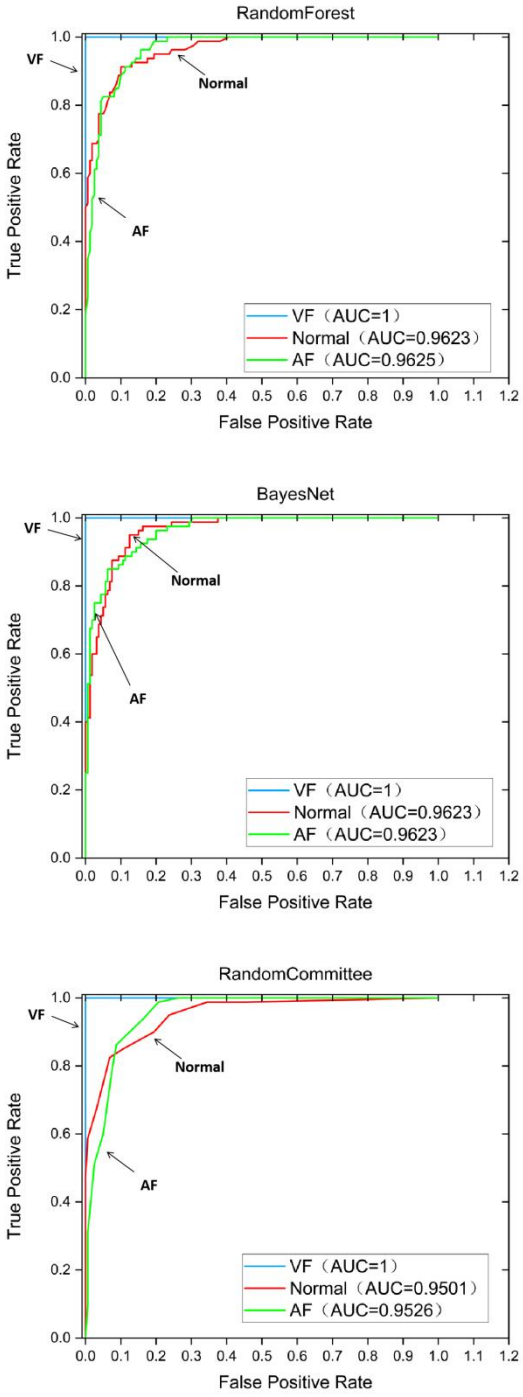

Fig. 10. The ROC curve of each machine learning

the comprehensive average absolute error is slightly inferior to the convolutional neural network.

The ROC curve of each machine learning is shown in Figure 10.

The ROC curve is all about receiver operating characteristics where each point on the curve reflects the sensitivity of stimuli to the same signal. It has a negative positive class rate on the X-axis and a positive class rate on the Y-axis. According to this curve, AUC, or the area under the ROC curve, is proposed, which can represent the effect of machine learning. The larger the AUC, the better the classification effect. According to the ROC curves of normal ECG signals, ventricular fibrillation ECG signals, and atrial fibrillation ECG signals by random forest, random committee,

TABLE V
PARAMETERS OF CLASSIFICATION RESULTS OF THE THREE METHODS

Feature extractor	Characteristic parameter	Characteristic parameter value
DWT	comprehensive Kappa	0.80
	comprehensive root relative square error	0.12
	comprehensive relative absolute error	0.28
	comprehensive root mean square error	0.25
	comprehensive average absolute error	0.55
CNN	comprehensive Kappa	0.86
	comprehensive root relative square error	0.08
	comprehensive relative absolute error	0.23
	comprehensive root mean square error	0.16
	comprehensive average absolute error	0.46
DSWOMP	comprehensive Kappa	**0.88**
	comprehensive root relative square error	**0.09**
	comprehensive relative absolute error	**0.14**
	comprehensive root mean square error	**0.18**
	comprehensive average absolute error	**0.28**

TABLE VI
THREE METHODS FEATURE DETECTION RESULTS

Feature extractor	classifier	Sample size	Recognition rate
DWT	Randomforest	80	84.58%
	Randomcommittee	80	80.42%
	BayesNet	80	82.50%
CNN	Randomforest	80	85.42%
	Randomcommittee	80	83.75%
	BayesNet	80	88.75%
DSWOMP	Randomforest	80	**90.42%**
	Randomcommittee	80	**87.92%**
	BayesNet	80	**89.17%**

and Bayesian network, it can be seen that random forest has the best classification effect on the features extracted by this algorithm. The curve area of the normal ECG signal is 0.9623, the curve area of ventricular fibrillation is 1, and the curve area of atrial fibrillation is 0.9625. According to the ROC curve, it can also be found that the algorithm extracted in this paper has a high recognition performance in recognizing ventricular fibrillation signals

As can be seen from Table VI, the recognition rate of DSWOMP in random forest, randomcommittee ,and Bayesian network classification methods is 90.42%, 87.92% ,and 89.17% respectively, and it can be seen that

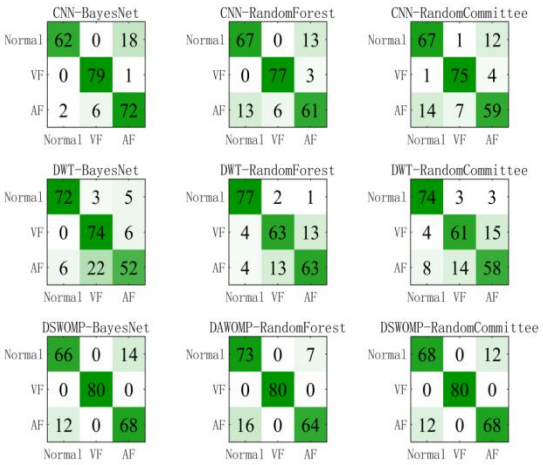

Fig. 11. Tripartite confusion matrix

TABLE VII
FEATURE TEST RESULT

classifier	Random forest	Randomcom mittee	BayesNet	Mean
Correctly classified Instances(%)	90.42	87.92	89.17	89.17
Kappa	0.86	0.82	0.84	0.84
Mean absolute error	0.14	0.12	0.07	0.11
Root mean squared error(%)	0.24	0.24	0.24	0.24
Relative absolute error	30.93	27.06	17.09	25.03
Root relative squared error(%)	50.28	49.95	49.85	50.03

DSWOMP has the highest recognition rate of 90.42% in randomforest classifier. The recognition rates of DWT in these three classification methods were 84.58%, 80.42% ,and 82.5%, respectively.The recognition rates of CNN in these three classification methods were 85.42%, 83.75% respectively.By comparison, it can be found that the DSWOMP algorithm has the best classification effect on the features extracted from the database in this paper. The confusion matrix of each classifier is shown in Figure 11.

According to the data in Table VII, the Kappa of random forest, randomcommittee, and Bayesian network is 0.86, 0.82, and 0.84 respectively, with an average value of 0.84, and Kappa is the smallest in the randomcommittee. The features extracted by the algorithm in this paper have high accuracy on the three classifiers, and the accuracy is the highest on the random forest. The minimum average absolute error of the three classifiers is 0.07, the average is 0.11, and the root-mean-square error of the three classifiers is 0.24. The average relative absolute error of the three classifiers is 25.03, and the root relative square error is 50.03%. Experiments show that the proposed algorithm has the best performance compared with convolutional neural networks and wavelet transform.

In addition, Precision, Recall, F-Measure, and ROC_Aera are also used as evaluation indexes of the algorithm. The Comparison bar chart of evaluation indexes under different machines is shown in Figure 12.Where Precision represents the proportion of cases that are positive in the examples that are classified as positive cases, it can also be said that Precision is the ability of the classifier not to label negative samples as positive. Recall, also known as recall rate, represents the proportion of the actual positive samples in the positive samples to the positive samples in the whole sample. F-Measure is also called comprehensive index. When there is a contradiction between Precision and Recall, we need to comprehensively evaluate Precision and Recall, so F-Measure is proposed. When the F-number is high, it indicates that the test method is effective and the results are in line with expectations. ROC_Aera compares the prediction results with the random guess results to obtain the true positive rate (TPR) and false positive rate (FPR) of the classification model under different thresholds. The larger the value of ROC_Aera, the better the performance of the classification model under different thresholds. Through the three bar graphs, we can see that the proposed algorithm has a good effect on the four parameters of Precision, Recall, F-Measure, and ROC_Aera. In the four parameters of random deep forest and random committee, the proposed algorithm is higher than the comparison algorithm. In a

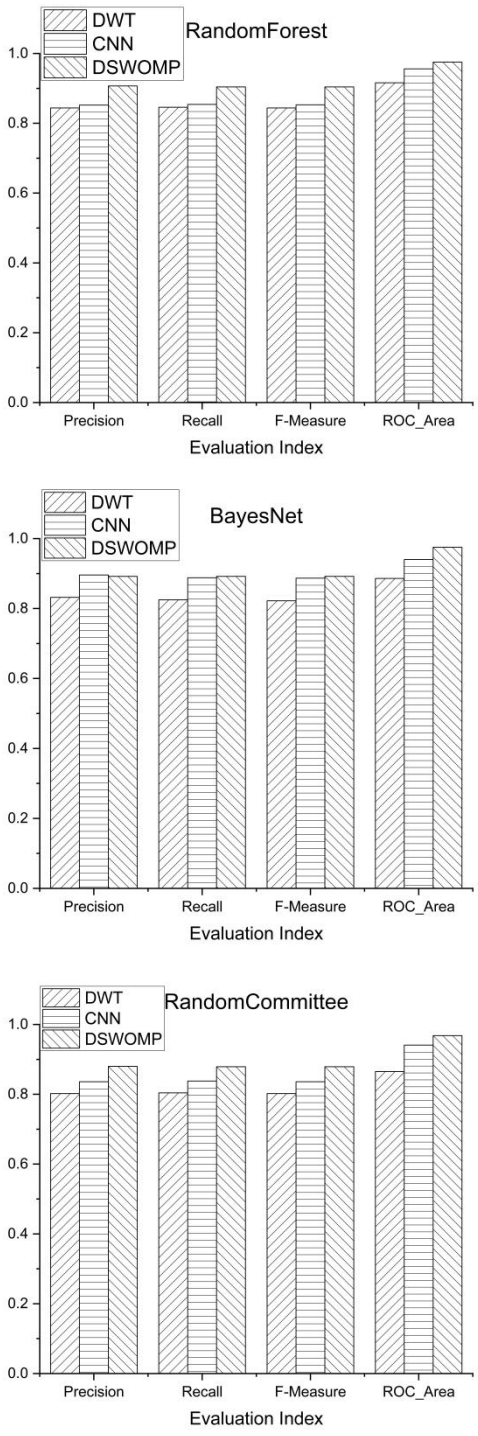

Fig. 12. Comparison bar chart of evaluation indexes under different machines

random deep forest, the Precision, Recall, F-Measure, and ROC_Aera of this algorithm are 0.907, 0.904, 0.904, and 0.975, respectively. On the Bayesian network, the Precision of the CNN algorithm is slightly higher than that of this algorithm, but the Recall is slightly lower than that of this algorithm. At this time, we must take comprehensive consideration. On F-Measure, we can see that this algorithm has higher recognition performance. The ROC_Aera of the algorithm in this paper is which is also the highest of all. By synthesizing all classifiers and all evaluation indexes, we can see that the proposed algorithm has higher performance in the process of ECG feature extraction.

VII. Summary and Outlook

In this paper, we proposed a feature extraction algorithm for ECG signals based on double-threshold segmented orthogonal matching tracking and K-singular-value decomposition. After the ECG signal is de-noised, a sample array is generated by the ECG signal and sent to the K-singular-value decomposition algorithm to update the supercomplete dictionary. Through iterative optimization, the reconstruction error rate of the ECG signal array is reduced, and the supercomplete dictionary is obtained. Then, this dictionary and an ECG signal sample array are sent to the double-threshold segmented orthogonal matching tracking algorithm for reconstruction. The sparse atomic matrix with the best reconstruction effect is ultimately selected, so as to obtain the characteristics of ECG signals. In this paper, three kinds of ECG signals are classified in addition to three pairs. A large number of experiments show that compared with the traditional ECG signal feature extraction algorithm, the algorithm extracted in this paper has the best recognition effect. According to the multi-classifier experiment, the average recognition rate and comprehensive recognition rate are defined in three groups of two classification experiments. Among the three algorithms, the comprehensive recognition rate of the algorithm proposed in this paper is the highest 93.96%. In addition, in the three-classification experiment, the proposed algorithm also has an absolute status recognition rate of 90.42%, ranking first. The experiment fully shows that the ECG signal features extracted by the double-threshold segmental sparse representation method have high recognition performance in the classification of normal, ventricular fibrillation, and atrial fibrillation.

The DSWOMP algorithm can be used to extract the features of normal, atrial fibrillation, and ventricular fibrillation ECG signals. Although some achievements have been made, there are many shortcomings. In the next step, the KSVD algorithm might be improved to obtain a dictionary matrix with a lower reconstruction failure rate, to improve the accuracy of ECG signal features in the classifier. By updating the algorithm, the difference between normal signals and the atrial fibrillation signals can be enhanced to improve the recognition rate. In addition, in our study we exclusively considered the steps of feature extraction. In future research, we will apply network learning and build an appropriate network to improve the recognition rate of the database.

References

[1] Rolant Gini John, K I Ramachandran, "Extraction of foetal ECG from abdominal ECG by nonlinear transformation and estimations," *Computer Methods and Programs in Biomedicine*, vol. 175, pp193-204, 2019.

[2] Kangming Chang, "Ensemble empirical mode decomposition for high frequency ECG noise reduction," *Biomedizinische Technik*, vol.55, no. 4, pp193-201, 2010.

[3] Siti Nurmaini, Bambang Tutuko, Muhammad Naufal Rachmatullah, Annisa Darmawahyuni, and Firdaus Firdaus, "Machine Learning Techniques with Low-Dimensional Feature Extraction for Improving the Generalizability of Cardiac Arrhythmia," *IAENG International Journal of Computer Science*, vol. 48, no.2, pp369-378, 2021.

[4] Khobragade Kalyani S, Deshmukh R.B, "ECG analysis using wavelet transforms," *IETE Journal of Research*, vol.43, no.6, pp423-432, 1997.

[5] Andres Hernandez-Matamoros, Hamido Fujita, Enrique Escamilla-Hernandez, Hector Perez-Meana, Mariko Nakano-Miyatake, "Recognition of ECG signals using wavelet based on atomic functions," *Biocyberntics and Biomedical Engineering*, vol.40, no.2, pp803-814, 2020.

[6] Sampath, A. , Sumithira, T.R, "ECG Morphological Marking using Discrete Wavelet Transform," *Intelligent Decision Technologies*, vol.10, no.4, pp373-383, 2017.

[7] Antoni Burguera, "Fast QRS Detection and ECG Compression Based on Signal Structural Analysis," IEEE Journal of Biomedical and Health Informatics, vol. 23, no. 1, pp123-131, 2019.

[8] Chouhan V. S., Mehta S. S., Lingayat N. S., "Delineation of QRS-complex, P and T-wave in 12-lead ECG," *International Journal of Computer Science and Network Security*, vol.8, no.4, pp185-190, 2008.

[9] Ruggero Donida Labati, Enrique Muñoz, Vincenzo Piuri, Roberto Sassi, Fabio Scotti, "Deep-ECG: Convolutional Neural Networks for ECG biometric recognition," *Pattern Recognition Letters*, vol.126, pp78-85, 2019.

[10] Mahfuz M. R. A., Moni M. A., Lio P., Islam S. M. S., Berkovsky S., Khushi M., Quinn J .M. W., "Deep convolutional neural networks based ECG beats classification to diagnose cardiovascular conditions," *Biomedical Engineering Letters*, vol.11, no.2, pp147-162, 2021.

[11] Sugondo Hadiyoso, Farell Fahrozi, Yuli Sun Hariyani, Mahmud Dwi Sulistiyo, "Image Based ECG Signal Classification Using Convolutional Neural Network," *International Journal of Online and Biomedical Engineering*, vol.18, no.4, pp64-78, 2022.

[12] Wang L. D., Zhou W., Xing Y., Liu N., Movahedipour M., Zhou X. G., "A novel method based on convolutional neural networks for deriving standard 12-lead ECG from serial 3-lead ECG," *Frontiers of Information Technology and Electronic Engineering* , vol.20, no.3, pp405-413, 2019.

[13] Xuan Hua, Jungang Han, Chen Zhao, Haipeng Tang, Zhuo He, Qinghui Chen, Shaojie Tang, Jinshan Tang, Weihua Zhou, "A Novel Method for ECG Signal Classification via One-Dimensional Convolutional Neural Network," *Multimedia Systems*, vol.28, no.4, pp1387-1399, 2020.

[14] Mehta S. S., Lingayat N. S., "Comparative Study of QRS Detection in Single Lead and 12-Lead Electrocardiogram using Support Vector Machine," *Engineering Letters*, vol.15, no.2, pp175-183, 2007.

[15] Mehta S. S., Lingayat N. S.,"Support Vector Machine for Cardiac Beat Detection in Single Lead Electrocardiogram," *IAENG International Journal of Applied Mathematics*, vol.36, no.2, pp20-26, 2007.

[16] Ramkumar Rathi, Niraj Yagnik, Soham Tiwari, and Chethan Sharma, "Analysis of Statistical Models for Fast Time Series ECG Classifications," *Engineering Letters*, vol. 30, no.2, pp718-729, 2022.

[17] Xiaohong Liang, Liping Li, Yuanyuan Liu, Dan Chen, Xinpei Wang, Shunbo Hu, Jikuo Wang, Huan Zhang, Chengfa Sun, Changchun Liu, "ECG_SegNet: An ECG delineation model based on the encoder-decoder structure," *Computers in Biology and Medicine*, vol.145, 105445, 2022.

[18] Aman Malali, Srinidhi Hiriyannaiah, Siddesh G.M., Srinivasa K.G., Sanjay N.T., "Supervised ECG wave segmentation using convolutional LSTM," *ICT Express*, vol.6, no.3, pp166-169, 2020.

[19] Abdolrahman Peimankar, Sadasivan Puthusserypady,"DENS-ECG: A Deep Learning Approach for ECG Signal Delineation," *Expert Systems with Applications,* vol.165, 113911, 2021.

[20] Debasish Jyotishi, Samarendra Dandapat, "An LSTM Based Model for Person Identification Using ECG Signal," *IEEE Sensors Letters*, vol.4, no.8, pp1-4, 2020.

[21] Aboli N. Londhe, Mithilesh Atulkar, "Semantic segmentation of ECG waves using hybrid channel-mix convolutional and bidirectional LSTM." *Biomedical Signal Processing and Control*, vol.63, 102162, 2020.

[22] Goldberger A. L.,Amaral L. A., Glass L., Hausdorff J. M., Ivanov P. C., Mark R. G., Mietus J. E., Moody G. B., Peng C. K., Stanley H. E., "PhysioBank, PhysioToolkit, and PhysioNet: components of a new research resource for complex physiologic signals," Circulation, vol. 101,no. 23, pp. E215-220, 2000.